Near-Wall Behavior of Separated and Reattaching Flows

William J. Devenport* and E. Peter Sutton†
Cambridge University, Cambridge CB2 1PZ, England, United Kingdom

Two separated and reattaching flows produced by a sudden expansion in a pipe have been studied experimentally. Velocity measurements were made close to the reattachment surface using a new type of pulsed-wire probe. These data show the near-wall flow to be very different from a normal turbulent boundary layer. Mean-velocity profiles do not obey the law of the wall and cannot be correlated outside the linear sublayer using the friction velocity. However, they do contain semilogarithmic regions that appear to form tangents to the linear sublayer profile. A satisfactory description of the backflow mean velocity profile is obtained by incorporating this observation into Simpson's model. The distribution of streamwise turbulence intensity in the near-wall region appears independent of the mean skin friction. It is, however, related to the root-mean-square of skin friction fluctuations expressed as a friction velocity. A simple one-dimensional model of the near-wall flow suggests that the form of the turbulence intensity profile is dependent on the frequency of large-scale velocity fluctuations.

Nomenclature

A = slope of the semilogarithmic region in mean-velocity profiles
A_1, A_2 = constants of integration
C_f = skin-friction coefficient based on U_{ref}
C_{f_N} = skin-friction coefficient based on U_N
$C_{f_{\text{rms}}}$ = coefficient of rms of skin-friction fluctuations, based on U_{ref}
C_{P_N} = nondimensional pressure gradient, $= [(\partial P/\partial X)N]/\frac{1}{2}\rho U_N^2$
k = amplitude of pressure-gradient fluctuations
N = distance from wall to location of peak mean backflow velocity
P = mean pressure
p = fluctuating pressure
R = radius of working-section pipe (75 mm)
Re_N = Reynolds number, $= N \cdot U_N/\nu$
St_r = Strouhal number, $= 2\pi\omega X_r/U_{\text{ref}}$
U = axial component of mean velocity
U_N = peak mean backflow velocity
U_{ref} = potential-flow velocity at separation
u = axial component of fluctuating velocity
u_τ = friction velocity based on mean wall-shear stress, $= \sqrt{\tau_w/\rho}$
u_τ^* = friction velocity based on rms of wall-shear-stress fluctuations, $= (\sqrt{\overline{\tau_w'^2}}/\rho)^{1/2}$
u^+ = U/u_τ
u^* = $\sqrt{\overline{u^2}}/u_\tau^*$
X = axial distance measured from separation
X_r = distance from separation to reattachment
Y = distance normal to wall
Y_1 = thickness of linear sublayer according to Eq. (6)
y^+ = Yu_τ/ν
y^* = Yu_τ^*/ν
δ_0 = "ac" boundary-layer thickness, $= \sqrt{(2\nu/\omega)}$
δ^* = $\delta_0 u_\tau^*/\nu$
ν = kinematic viscosity
ρ = density
τ_w = mean wall shear stress
τ_w' = fluctuating wall shear stress
ω = angular frequency

Introduction

MOST incompressible turbulent separated and reattaching flows consist of a shear layer that on one side bounds a main stream and on the other encloses a region of time-mean backflow next to a wall. In all such flows, there is a thin region adjacent to the reattachment surface within which the latter has a direct influence on the flow. This near-wall region is often thought of as extending from the wall to the vicinity of the peak time-mean backflow velocity.

Past experimental work has shown that the near-wall flow lacks many characteristics normally associated with turbulent boundary layers: Profiles of turbulence intensity in the near-wall region do not have a peak close to the wall[1-3]; profiles of mean velocity do not contain log-law regions related to the friction velocity u_τ in the normal way[1,3-6]; the Reynolds shear stress remains small in the near-wall region[4,7,8]; and turbulent bursts (the rapid mixing of fluid from the viscous sublayer that has been lifted away from the wall) are relatively infrequent.[9] Consistent with these results, there is little production or convection of turbulence kinetic energy within the near-wall region.[5,7] Turbulence energy dissipated here appears to be supplied primarily by diffusion from the separated or reattaching shear layer above.

The lack of much Reynolds shear stress suggests the laminar shear stress $\mu\partial U/\partial Y$ is important. When based on the local peak backflow velocity and the distance from the wall at which it occurs, the low Reynolds numbers (Re_N) and high skin-friction coefficients (C_{f_N}) of the near-wall flow also suggest a laminar-like structure. The C_{f_N} and Re_N are typically 500 and 0.02 respectively.[3,9-11]

The intensity of velocity fluctuations parallel to the wall in the near-wall region is of the order of magnitude of the local mean velocity.[4,9,12] The intensity of fluctuations normal to the wall is nearly an order of magnitude smaller.[2] The characteristic frequency of velocity fluctuations parallel to the wall is comparatively low. Spectra measured by Adams et al.[9] show peaks at Strouhal numbers, based on the distance from separation to reattachment (X_r) and the potential-flow velocity at separation (U_{ref}), of between 0.2 and 0.5. Diagrams presented by Eaton and Johnston[13] showing the flow direction at the wall, close to the reattachment point, suggest a Strouhal num-

Received June 9, 1989; revision received and accepted for publication Nov. 15, 1989.

*Graduate Student, Engineering Department; currently, Assistant Professor, Department of Aerospace and Ocean Engineering, Virginia Polytechnic Institute and State University, Blacksburg, VA. Senior Member AIAA.

†Lecturer, Engineering Department; currently retired.

ber of about 0.3. Simpson et al.[5] also observe some low-frequency velocity fluctuations.

The work just referenced by no means gives a complete picture of the near-wall flow. Many basic questions remain. How, for example, does the turbulence structure of the near-wall flow depend on the separated or reattaching shear layer above? What are the best parameters for describing the time-averaged and turbulence structure? Do useful laws for those scaling parameters exist? This lack of understanding results primarily from a dearth of experimental data. Measurements in the near-wall region are difficult to make; it is usually too thin to be probed using standard pulsed-wire or laser-Doppler anemometers, and the flow here is too turbulent for more conventional techniques to be used.

A new type of pulsed-wire probe, designed specifically for use in the near-wall regions of separated flows, has recently been developed.[14] The purpose of this paper is to present and discuss detailed measurements made with this probe in the light of the questions just raised. Measurements were made in two separated and reattaching flows formed downstream of an axisymmetric backward-facing step. This research forms part of a longer-term study of axisymmetric separated flows.[12,15,16]

Apparatus

The experimental apparatus outlined below is described in more detail by Devenport.[16]

Wind Tunnel

A small axisymmetric wind tunnel built for earlier experiments on separation bubbles[12,15] was used. This has a cylindrical settling chamber 840 mm in diameter. Air is supplied to the chamber from a centrifugal blower through a flexible pipe, a silencer, a wide-angle diffuser with screens, further screens with fine mesh, and a honeycomb. Air from the chamber passes through a nozzle into the working section (see Fig. 1). The nozzle consists of a contracting section with a throat diameter of 80 mm followed by a parallel-sided section 80 mm in diameter and 240 mm in length. A boundary-layer transition trip, 1 mm high with a rectangular cross section, is mounted 180 mm upstream of the nozzle exit.

Under nominal test conditions, the flow at the nozzle exit consists of a uniform potential core with a mean velocity U_{ref} of 15 m/s and an axial turbulence intensity of 0.4%. This is surrounded by a near-equilibrium turbulent boundary layer 7 mm thick of momentum-thickness Reynolds number 6.6×10^2; the Reynolds number per meter is 1.0×10^6.

The working section, a 150-mm-diam pipe, is attached to the downstream end of the nozzle. The sudden axisymmetric expansion from the nozzle to the working-section pipe (step height 35 mm) causes the flow to separate and then reattach to the pipe wall downstream. This "datum" flow may be modified by mounting a centerbody in the working section. The centerbody, included in Fig. 1, imposes a strong negative streamwise pressure gradient on the reattaching flow in the working section. Its shape was computed using a potential-flow method to give an approximation to a specified pressure distribution. The exact shape and details of the design of the centerbody are given by Devenport.[16] When in use, the centerbody is mounted with its upstream end 90 mm downstream of the nozzle exit.

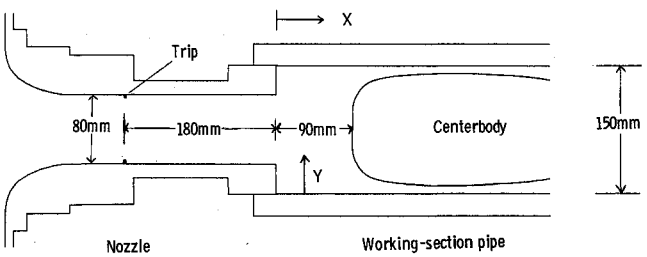

Fig. 1 Cross section of the nozzle and working-section pipe.

Instrumentation

Pulsed-wire techniques were used extensively. A pulsed-wire anemometer measures velocity or skin friction by timing the flight of a heated tracer of air between a pulsing wire and one of two sensor wires. Three different types of probes were used. All were operated using a PELA Flow Instruments Ltd. anemometer unit interfaced to a Commodore CBM 4032 (PET) computer. The operating principles of this unit are described by Bradbury and Castro.[17]

For velocity measurements more than 6 mm from the working section wall, a PELA pulsed-wire probe of standard design[17] was used. It consists of two parallel sensor wires mounted perpendicular to and on either side of a central pulsing wire at the end of a probe stem. The pulsing and sensor wires have lengths of 8 mm and are made from tungsten wire of 9 and 2.5μ diam, respectively. The large size of this probe prevents it from being used in the near-wall region.

For velocity measurements in the near-wall region, a new type of pulsed-wire probe was used. The design and testing of the probe are only summarized here; for more details see Devenport et al.[14] The probe (see Fig. 2) is built around a plug cast from epoxy resin. When mounted, the top surface of the plug lies flush with the internal wall of the working-section pipe and is thus curved with a 75 mm radius. The wires are arranged so that the probe is sensitive to the axial velocity component U. The pulsing wire (8-mm long, 9-μ-diam tungsten) rises vertically out of the plug center to which it is fixed. The two sensor wires (8-mm long, 5-μ-diam tungsten) are mounted horizontally on either side, across the curved surface of the plug. The sensor wires and their supporting prongs can be traversed in the vertical direction using a micrometer screw allowing velocity measurements made between 0.15 and 5.5 mm from the wall. Bias errors in measurements made with this probe, analyzed by Devenport et al.,[14] are no greater than for a standard pulsed-wire probe. Comparisons with a hot-wire anemometer in an attached turbulent boundary layer suggest the near-wall probe measures mean-velocity and turbulence intensity to accuracies of 2 and 10%, respectively.

For measurements of wall-shear stress, a pulsed-wire skin-friction probe supplied by PELA was used. This probe, described by Castro and Dianat,[18] consists of three parallel wires mounted approximately 0.05 mm from the wall. The central pulsing wire is 3-mm long and made from 9-μ-diam tungsten wire. The two sensor wires are 2-mm long and made from

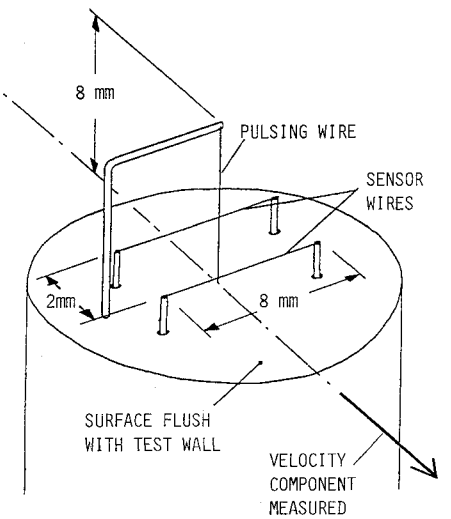

Fig. 2 Near-wall pulsed-wire probe.

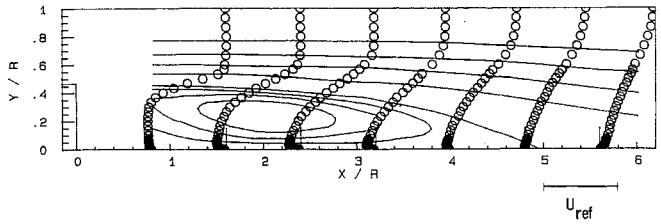

Fig. 3 Mean axial velocity profiles and mean streamlines for the datum flow.

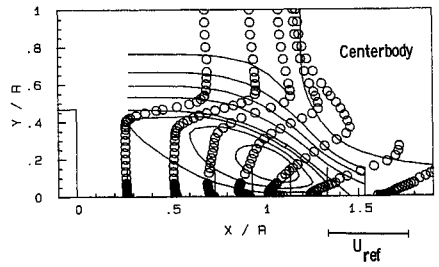

Fig. 4 Mean axial velocity profiles and mean streamlines for the flow with centerbody.

2.5-μ-diam tungsten wire. The probe measures velocity in the sublayer, which is assumed to be proportional to skin friction.

Pulsed-wire probes must be calibrated since the relationship between velocity or skin friction and the reciprocal of the time of flight is nonlinear. This is due to the effects of thermal diffusion on heat tracers.[19] The standard and near-wall pulsed-wire probes (which had qualitatively identical calibration curves) were calibrated for velocity in the potential core at the nozzle exit. The velocity here was known from pressure measurements and could be varied by altering the blower speed. The pulsed-wire skin-friction meter was calibrated for wall shear stress in equilibrium turbulent boundary layer in an against a Preston tube. For all probes, the calibration curve was approximated by a series of straight line segments joining the measured calibration points. This was found to give a more accurate representation of the calibration curve than the analytical expressions used by Bradbury,[19] Castro and Dianat,[18] and others.

Results and Discussion

Results are presented using the coordinate system shown in Fig. 1. Figures 3 and 4 show profiles of time-mean velocity and time-averaged streamlines deduced from them. Figure 5 shows distributions of the mean and root-mean-square (rms) skin-friction coefficients $C_f (= \tau_w / \frac{1}{2}\rho U_{ref}^2)$ and $C_{f_{rms}} (= \sqrt{\overline{\tau_w^2}} / \frac{1}{2}\rho U_{ref}^2)$.

In both cases the flow separates at the sudden expansion creating a turbulent shear layer, which then reattaches to the pipe wall downstream. In the datum flow (without the centerbody), the distance from separation to reattachment is $5 \pm 0.13R$ (10.7 step heights). (All uncertainty intervals were calculated for 95% confidence limits using the method of Kline and McClintock.[20]) With the centerbody, X_r is $1.47 \pm 0.04R$ (3.14 step heights). Mean reattachment positions were measured as the point of zero time-mean skin friction using the pulsed-wire skin-friction meter. In the datum flow, circumferential variations in X_r were less than $\pm 2.5\%$.

The mean velocity profiles of the two flows show the large velocity gradient associated with the separated shear layer and its relaxation with distance downstream. They also show the development of the mean backflow. Time-averaged backflow velocities reach a maximum of $-0.16U_{ref}$ in the datum flow at $X/X_r = 0.48$ and one of $-0.27U_{ref}$ at $X/X_r = 0.77$ with the centerbody.

Figure 5 demonstrates that the distributions of C_f and $C_{f_{rms}}$ (uncertainties both $\pm 6\%$) do not scale on the distance to reattachment. In the datum flow, C_f reaches a minimum of

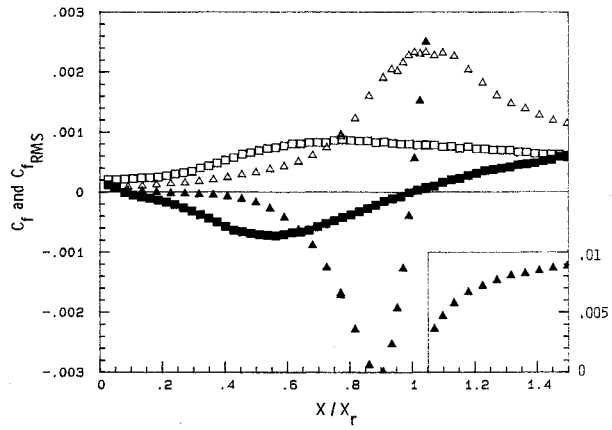

Fig. 5 Skin-friction distributions for the datum flow (squares) and the flow with centerbody (triangles); solid symbols, C_f; open symbols, $C_{f_{rms}}$.

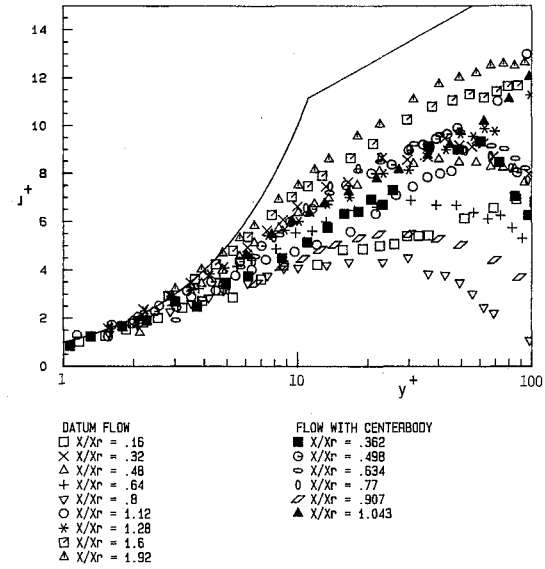

Fig. 6 Near-wall mean-velocity profiles plotted in inner variables.

-0.00073 (-0.03 based on local peak backflow velocity) approximately midway between separation and reattachment. With the centerbody, the minimum occurs at $X/X_r = 0.9$ where C_f is -0.0030 (-0.05 based on local backflow conditions). In both flows, $C_{f_{rms}}$ reaches its maximum near reattachment. The peak value of $C_{f_{rms}}$ is, however, about 2.5 times as large with the centerbody than without.

The structure of these flows, in particular the turbulence structure of the separated and reattaching shear layers, is discussed in detail by Devenport.[16] In this paper, we shall restrict our attention to their near-wall behavior upstream of reattachment and in the reattachment region. To allow comparisons to be made with the results of other workers, we shall treat these flows as though they were plane two-dimensional in the time mean. Axisymmetric effects would have been small as both near-wall regions were thin in comparison to the pipe radius.

Profiles of Time-Mean Velocity

It is conventional to scale near-wall velocity measurements using the friction velocity $u_\tau = \sqrt{\tau_w/\rho}$. Upstream of reattachment, mean-velocity profiles may also be normalized using the local peak backflow velocity U_N and the distance from the wall at which it occurs, N.

Profiles of mean-velocity (uncertainty $\pm 2.5\%$) measured in both flows are plotted in terms of $u^+ (= U/u_\tau)$ and $y^+ (= Yu_\tau/\nu)$ in Fig. 6 (u_τ being obtained from the independent skin-friction measurements of Fig. 5). The two lines on

this figure represent the linear and semilogarithmic regions of a standard turbulent boundary-layer velocity profile:

$$u^+ = y^+ \tag{1}$$

$$u^+ = 2.4 \ln y^+ + 5.4 \tag{2}$$

In the sublayer (which at some locations is thinner than $3y^+$), the profiles follow the $u^+ = y^+$ line, as they should. However, as would be expected from the results of previous investigations, there is no collapse of the data outside the sublayer. While most profiles have semilogarithmic regions here, these fall well below Eq. (2) and appear to form tangents to the linear sublayer profile.

Figure 7 shows those profiles measured upstream of reattachment plotted in terms of U/U_N and Y/N. Considering the uncertainty in the data (which is worst near separation), Fig. 7 does show some collapse, particularly over the outer part of the profiles ($Y/N > 0.6$).

For Figs. 6 and 7 to be consistent, there must either be a simple constant of proportionality between U_N and u_τ and between N and ν/u_τ or some change in scaling of the velocity profile between the linear sublayer and the outer part of the near-wall region. The first of these possibilities leads to the expression

$$\frac{U_N}{u_\tau} = K \frac{N u_\tau}{\nu} \tag{3}$$

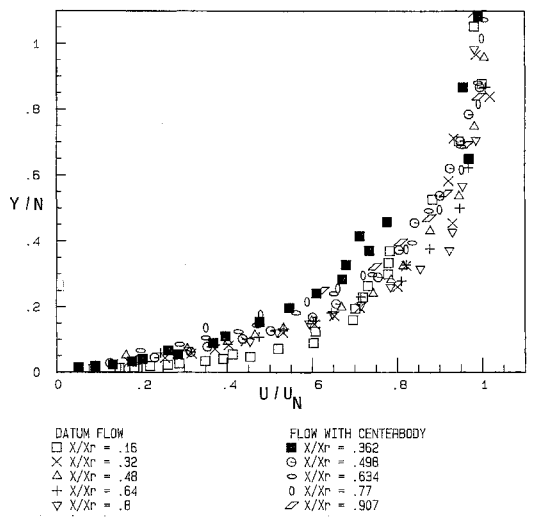

Fig. 7 Normalized backflow mean-velocity profiles.

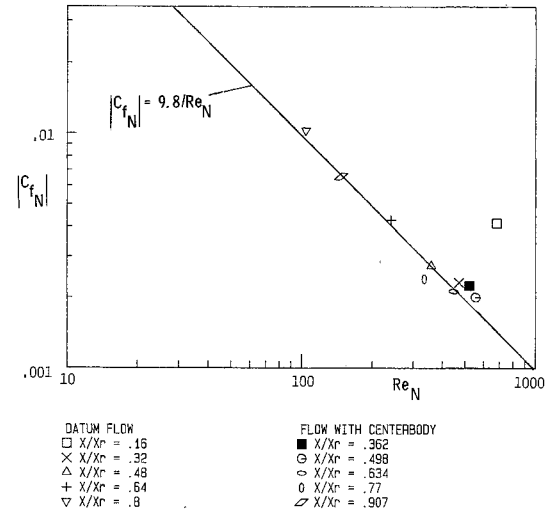

Fig. 8 Local skin friction coefficient as a function of local backflow Reynolds number.

where K is a universal constant. Rearranging gives

$$C_{f_N} = 2(K \cdot Re_N)^{-1} \tag{4}$$

where $C_{f_N} (= \tau_w / \frac{1}{2}\rho U_N^2)$ and Re_N represent the local skin-friction coefficient and Reynolds number of the backflow. Although estimates of C_{f_N} and Re_N obtained from the present measurements appear consistent with this relationship (see Fig. 8), the results of other investigations are not. The data of Adams and Johnston,[1] Eaton and Johnston,[13] and Driver and Seegmiller,[21] presented by Adams and Johnston,[1] more closely follow a relationship of the form

$$C_{f_N} \sim Re_N^{-\frac{1}{2}} \tag{5}$$

In general, then, there is a change in scaling. Any universal description of the backflow velocity profile must therefore depend on N, U_N, and u_τ. One such description has been proposed by Simpson.[22] Close to the wall, Simpson uses a sublayer profile, scaled on u_τ, that includes the effect of the mean streamwise pressure gradient $\partial P/\partial X$

$$u^+ = y^+ + \frac{\partial P}{\partial X}\frac{\nu}{2\rho u_\tau^3} y^{+2} \qquad \text{for } 0 < Y < Y_1 \tag{6}$$

He arbitrarily chooses the sublayer thickness Y_1 to be 2% of the thickness of the near-wall region N. Away from the wall, Simpson uses an expression that scales on N and U_N,

$$\frac{U}{|U_N|} = A\left[\frac{Y}{N} - \log\left(\frac{Y}{N}\right) - 1\right] - 1 \qquad \text{for} \quad Y > Y_1 \tag{7}$$

where A is an empirical constant. Consistent with the present results, this expression has a partly semilogarithmic behavior. Simpson shows a semilogarithmic region to be an implicit result of the change in scaling. Figure 9 compares the present measurements with Eq. (7). Curves for $A = 0.3$ (as suggested by Simpson's measurements) and $A = 0.235$ (as suggested by those of Castro and Dianat[6]) are drawn. Quantitatively, the agreement is fairly poor. For $Y > N$ the mean-velocity profiles do not collapse, making Eq. (7) inadequate here. For $Y < N$ the agreement is better, but most of the measured profiles lie significantly above the analytical curves. Qualitatively, however, the profile shape is well described by Eq. (7). It appears that the agreement would be much better if A were allowed to take different values.

The fact the A does not appear to be a universal constant can be easily accounted for by extending Simpson's[22] relations. The semilogarithmic regions in the present mean-veloc-

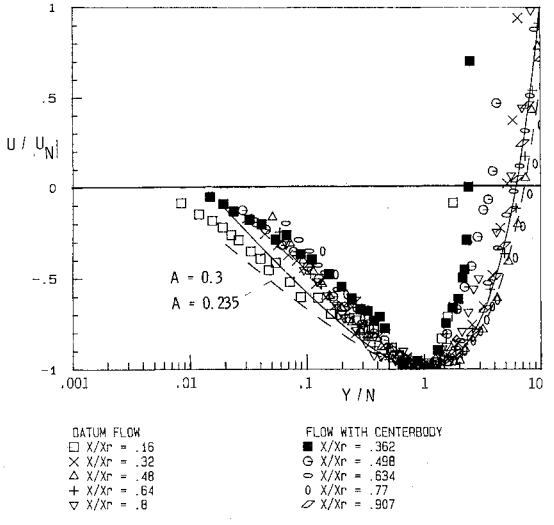

Fig. 9 Normalized backflow mean-velocity profiles compared with Eq. (7).

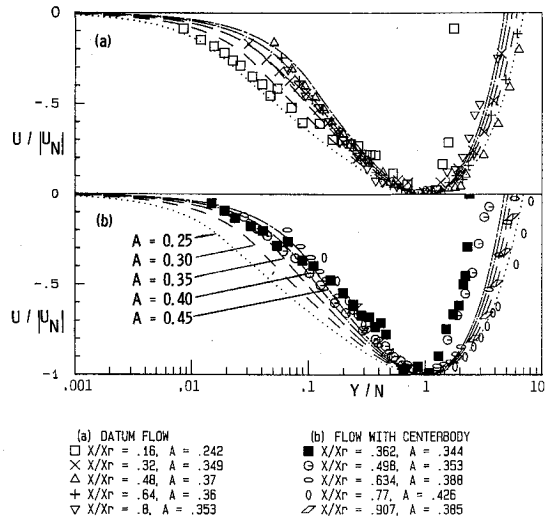

Fig. 10 Normalized backflow mean-velocity profiles compared with a family of curves given by Eqs. (6), (7), (10), and (11): a) datum flow; b) flow with centerbody.

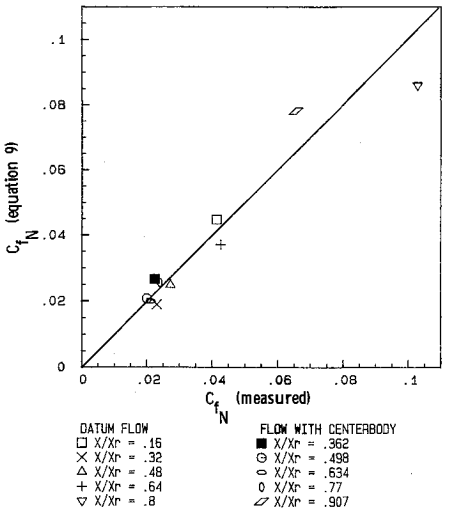

Fig. 11 Comparison of measured values of C_{f_N} and estimates obtained using Eq. (11).

ity profiles (see Fig. 6) all appear to form tangents to the linear sublayer profile suggesting that Eq. (7) should be tangent to Eq. (6) at Y_1. This matching gives an implicit equation for the position Y_1

$$0 = \left(C_{f_N} + C_{P_N}\frac{Y_1}{N}\right)\ell n\left(\frac{Y_1}{N}\right) + \left[\frac{1}{2}C_{P_N}\frac{Y_1}{N} - \left(\frac{1}{2}Re_N\frac{Y_1}{N}\right)^{-1}\right]\left(1 - \frac{Y_1}{N}\right) \tag{8}$$

where the equation for the slope A is

$$A = \frac{\frac{1}{4}C_{P_N}Re_N(Y_1/N)^2 - 1}{\ell n\,(Y_1/N)} \tag{9}$$

Simpler expressions are obtained if the pressure-gradient term is negligible (as it was in the present experiments). These are

$$0 = \frac{1}{2}C_{f_N}Re_N\frac{Y_1}{N}\ell n\left(\frac{Y_1}{N}\right) + \frac{Y_1}{N} - 1 \tag{10}$$

$$C_{f_N} = -2A(e^{1/A} - 1)/Re_N \tag{11}$$

Equations (6), (7), (10), and (11) describe, without empirical constants, a mean-velocity profile determined by C_{f_N} and Re_N.

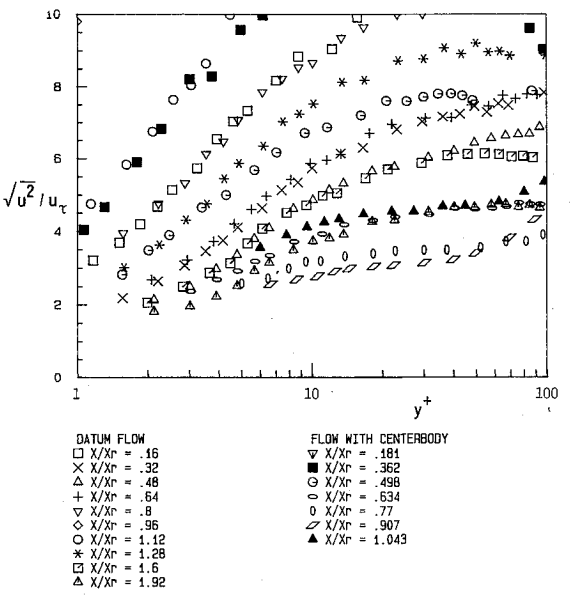

Fig. 12 Near-wall turbulence-intensity profiles plotted in inner variables.

Plotted in terms of Y/N and U/U_N, the profile shape depends only on the value of A. A series of these curves for different values of A are compared with the present measurements in Fig. 10. Values of A obtained from measurements of C_{f_N} and Re_N are included in the legends of this figure.

For $Y > N$, there are still large discrepancies between the measured and theoretical profiles. For $Y < N$, the agreement is better than before but most of the measured profiles still lie slightly above their corresponding analytical ones, particularly in the flow with the centerbody. At most locations, however, this difference is smaller than the uncertainty in the measurements.

Perhaps the most important result of the preceding analysis is Eq. (11). This amounts to a skin-friction law since it gives local skin-friction coefficient as a function of the slope of the semilogarithmic part of the mean-velocity profile (A) and the local Reynolds number. The validity of this relationship is examined in Fig. 11 in which measured values of C_{f_N} are compared with values computed using Eq. (11) from the measured slopes and Reynolds numbers. Considering the uncertainties involved (especially in determining the value of A), Fig. 11 shows a satisfactory correlation.

Profiles of Turbulence Intensity

In this section, the axial turbulence intensity measurements made with the near-wall pulsed-wire probe are discussed separately from those of mean velocity just presented. The justification for this comes from the turbulence kinetic energy equation. Simpson et al.[5] and Pronchick and Kline[7] have shown that the production and convection terms of this equation are insignificant in the near-wall region. Without these terms, turbulence kinetic energy ceases to be dependent on the local mean-velocity field. An illustration of this is Fig. 12. Here the near-wall profiles of axial turbulence intensity $\sqrt{\overline{u^2}}$ (uncertainty $\pm$ 10%) are plotted in terms of $\sqrt{\overline{u^2}}/u_\tau$ and y^+. Even at low values of y^+, u_τ (a factor determined by the mean-velocity field) does not scale these profiles.

A scaling parameter directly related to the turbulence field is clearly required. One candidate is the friction velocity based on the intensity of wall shear-stress fluctuations, $(\sqrt{\overline{\tau'^2}}/\rho)^{0.5}$, which we shall represent using the symbol u_τ^*. Figure 13 presents the data replotted in terms of $u^*(=\sqrt{\overline{u^2}}/u_\tau^*)$ and y^* $(=Yu_\tau^*/\nu)$. The profiles measured in the datum flow now collapse reasonably well to a single curve. Those measured with the centerbody also collapse (except at $X/R = 1.33$) but onto a different curve. The implications of this behavior are

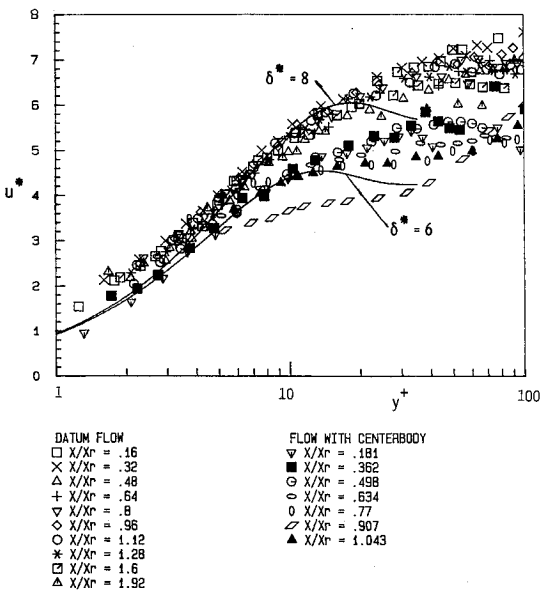

Fig. 13 Near-wall turbulence-intensity profiles plotted in terms of u^* and y^* and compared with Eq. (18).

best revealed by considering a simple theoretical model of the near-wall flow.

As a first approximation, we will ignore all but the U component of velocity in the near-wall region. The equations of motion are then

$$\frac{\partial u}{\partial t} = -\frac{1}{\rho}\frac{\partial p}{\partial X} + \nu\frac{\partial^2 u}{\partial Y^2} \tag{12}$$

Though drastic, this assumption is not entirely unrealistic. Previous work (already described) has shown the near-wall flow to be dominated by large-amplitude low-frequency velocity fluctuations parallel to the wall. Equation (12) is also consistent with Simpson's[23] proposal that large-scale velocity fluctuations in the near-wall region are driven primarily by fluctuations in streamwise pressure gradient produced by the separated and reattaching shear layer above. Consider a single frequency ω of pressure-gradient fluctuations of amplitude k, i.e.,

$$-\frac{1}{\rho}\frac{\partial p}{\partial X} = k\exp(i\omega t) \tag{13}$$

[Since Eq. (12) is linear, solutions for different frequencies may be superimposed.] The general solution to Eq. (12) is then

$$u = A_1\exp[i(\omega t - Y/\delta_0) - Y/\delta_0] + A_2\exp[i(\omega t + Y/\delta_0) + Y/\delta_0] + (k/i\omega)\exp(i\omega t) \tag{14}$$

where δ_0 is sometimes called the ac boundary-layer thickness. For a physically realistic solution, the constant of integration A_2 must be taken as zero; otherwise $u \to \infty$ as $Y \to \infty$. The A_1 is evaluated by applying the no-slip condition $u = 0$ at $Y = 0$. Extracting the real part of Eq. (14) then leaves

$$u = (k/\omega)\,[\sin(\omega t) - \exp(-Y/\delta_0)\sin(\omega t - Y/\delta_0)] \tag{15}$$

This is a fairly well-known solution to the equations of motion that has been used in the past to describe oscillating laminar flows.[24,25] We will use it here to obtain an equation for the turbulence intensity. Taking the root-mean-square gives

$$\sqrt{\overline{u_2}} = (k/\omega)\,[0.5 + 0.5\exp(-2Y/\delta_0) - \exp(-Y/\delta_0)\cos(Y/\delta_0)]^{0.5} \tag{16}$$

The parameter u_τ^* may be obtained from the gradient of Eq. (15) at the wall

$$u_\tau^* = \frac{\sqrt{\overline{\tau'^2_w}}}{\rho} = \frac{k\nu}{\rho\omega\delta_0} \tag{17}$$

Using the nondimensional variables u^* and y^* already defined and by defining δ^* as $\delta_0 u_\tau^*/\nu$, Eq. (16) becomes

$$u^* = \delta^*[0.5 + 0.5\exp(-2y^*/\delta^*) - \exp(-y^*/\delta^*)\cos(y^*/\delta^*)]^{0.5} \tag{18}$$

In these idealized circumstances then, the profile of turbulence intensity is a function of y^* and the nondimensional parameter δ^*, dependent on the frequency of fluctuations. Curves described by Eq. (18) are compared with the present measurements in Fig. 13. For $y^* < 10$, there is reasonable agreement between Eq. (18) and the measurements if δ^* is taken as 8 in the datum flow and as 6 in the flow with the centerbody. For $y^* > 10$, the agreement is not as good because of a peak in the theoretical profiles. This peak appears to be a result of the choice of a single frequency to represent the fluctuating pressure gradient. Through superposition, a range of frequencies would tend to smooth out this feature resulting in a more realistic curve. Ignoring this discrepancy we appear to have, in the datum flow,

$$\delta^* = \frac{\delta_0 u_\tau^*}{\nu} = \sqrt{\frac{2u_\tau^{*2}}{\omega\nu}} = \sqrt{\frac{C_{f_{\text{rms}}}}{\omega\nu}}\,U_{\text{ref}} \approx 8 \tag{19}$$

which implies a frequency of velocity fluctuations in the near-wall region, in terms of Strouhal number based on reference velocity and bubble length ($St_r = \omega X_r/2\pi U_{\text{ref}}$), of 0.18 near separation and 0.74 near reattachment. For the flow with the centerbody, it appears that

$$\delta^* = \sqrt{\frac{C_{f_{\text{rms}}}}{\omega\nu}}\,U_{\text{ref}} \approx 6 \tag{20}$$

which implies $St_r = 0.05$ near separation and 1.12 near reattachment.

The preceding frequencies are similar in magnitude to those observed by previous workers studying the near-wall behavior of separated flows. The increase in frequency from separation to near reattachment, implied by the rather variations of $C_{f_{\text{rms}}}$ (see Fig. 5), is also supported by the sparse information available from previous work. It is, of course, the opposite of what would be expected if fluctuations in the near-wall flow were determined entirely by the passing of eddies in the shear layer above. Velocity spectra measured by Adams et al.,[9] in the near-wall flow downstream of a backward-facing step, show an increase in the characteristic frequency of velocity fluctuations (St_r) from 0.2 to 0.5 between $X/X_r = 0.38$ and 0.58. Spectra of wall-pressure fluctuations measured by Cherry,[26] under the separation bubble formed in the flow over a blunt flat plate, show a peak at $St_r = 0.1$ near separation and one at $St_r = 0.6$ near reattachment. Cherry attributes the first of these to a slow "flapping" of the separated shear layer and the second to the passing of shear-layer eddies through the reattachment region. Both of these processes are likely to be associated with velocity fluctuations in the near-wall region of the same frequency.

A further result of the preceding analysis, implied by Eqs. (19) and (20) and the collapse of the turbulence profiles in Fig. 13, is that $\omega\nu/u_\tau^{*2}$ is an appropriate nondimensional frequency for fluctuations in the near-wall flow. This is analogous to the nondimensional frequency $\omega\nu/u_\tau^2$ usually used in "normal" turbulent boundary layers.

Conclusions

The near-wall behavior of two separated and reattaching flows formed by a sudden expansion in a pipe has been studied

experimentally. Pulsed-wire techniques were used extensively. A new "near-wall" pulsed-wire probe was used to measure detailed profiles of velocity and turbulence intensity in those regions of reversing flow close to the pipe wall.

This near-wall flow is very different from a normal attached turbulent boundary layer. Mean velocity profiles do not obey the law of the wall and cannot be correlated outside of the linear sublayer using the friction velocity. However, they do contain semilogarithmic regions that appear to form tangents to the linear sublayer profile. A satisfactory description of the backflow mean velocity profile is obtained by incorporating this observation into Simpson's[22] model. This extension also leads to an expression for the local skin-friction coefficient in terms of the local Reynolds number of the backflow and the slope of the semilogarithmic part of the profile. This skin-friction law is consistent with the present data.

The distribution of streamwise turbulence intensity produced by the near-wall flow appears independent of the time-mean skin friction. It is, however, related to the rms of fluctuations in skin friction expressed as a friction velocity. A simple one-dimensional model of the near-wall flow has been proposed in which the streamwise velocity fluctuations of the near-wall flow are driven by pressure gradient fluctuations imposed by the shear layer above. This model suggests that the form of the turbulence intensity profile is a function of a parameter δ^* dependent on the frequency of velocity fluctuations in the near-wall flow.

With appropriate values of δ^*, the theory satisfactorily describes the form of the turbulence intensity profile close to the wall. These values of δ^* imply characteristic frequencies in the near-wall flow typical of those reported by other workers.

References

[1]Adams, E. W., and Johnston, J. P., "Flow Structure in the Near-Wall Zone of a Turbulent Separated Flow," *AIAA Journal,* Vol. 26, No. 8, 1988, pp. 932–939.

[2]Shiloh, K., Shivaprasad, B. G., and Simpson, R. L., "The Structure of a Separating Turbulent Boundary Layer, Part 3. Traverse Velocity Measurements," *Journal of Fluid Mechanics,* Vol. 113, 1981, pp. 75–90.

[3]Ruderich, R., and Fernholz, H. H., "An Experimental Investigation of a Turbulent Shear Flow with Separation, Reverse Flow, and Reattachment," *Journal of Fluid Mechanics,* Vol. 163, pp. 283–322.

[4]Simpson, R. L., Chew, Y.-T., and Shivaprasad, B. G., "The Structure of a Separating Turbulent Boundary Layer. Part 1. Mean Flow and Reynolds Stresses," *Journal of Fluid Mechanics,* Vol. 113, 1981, pp. 23–51.

[5]Simpson, R. L., Chew, Y.-T., and Shivaprasad, B. G., "The Structure of a Separating Turbulent Boundary Layer. Part 2. Higher Order Turbulence Results," *Journal of Fluid Mechanics,* Vol. 113, 1981, pp. 53–73.

[6]Dianat, M., and Castro, I. P., "Measurements in Separating Boundary Layers," *AIAA Journal,* Vol. 27, No. 6, 1989, pp. 719–724.

[7]Pronchick, S. W., and Kline, S. J., "An Experimental Investigation of the Structure of Turbulent Reattaching Flow Behind a Backward-Facing Step," Dept. of Mechanical Engineering, Stanford Univ., Stanford, CA, Rept. MD-42, 1983.

[8]Stevenson, W. H., Thompson, H. D., and Craig, R. R., "Laser Velocimeter Measurements in Highly Turbulent Recirculating Flows," *Journal of Fluids Engineering, Transactions of the ASME,* Vol. 106, 1984, pp. 173–180.

[9]Adams, E. W., Johnston, J. P., and Eaton, J. K., "Experiments on the Structure of a Turbulent Reattaching Flow," Dept. of Mechanical Engineering, Stanford Univ., Stanford, CA, Rept. MD-43, 1984.

[10]Westphal, R. V., Johnston, J. P., and Eaton, J. K., "Experimental Study of Flow Reattachment in a Single-Sided Sudden Expansion," Dept. of Mechanical Engineering, Stanford Univ., Stanford, CA, Rept. MD-41, 1984.

[11]Castro, I. P., and Haque, A., "The Structure of a Turbulent Shear Layer Bounding a Separation Region," *Journal of Fluid Mechanics,* Vol. 179, 1987, pp. 439–468.

[12]Evans, G. P., "Separation Bubble at Pipe Entrance," Ph.D. Dissertation, Cambridge Univ., Cambridge, England, UK, 1973.

[13]Eaton, J. K., and Johnston, J. P., "Turbulent Flow Reattachment: An Experimental Study of the Flow and Structure Behind a Backward-Facing Step," Dept. of Mechanical Engineering, Stanford Univ., Stanford, CA, Rept. MD-39, 1980.

[14]Devenport, W. J., Evans, G. P., and Sutton, E. P., "A Traversing Pulsed-Wire Probe for Velocity Measurements Near a Wall," *Experiments in Fluids*, Vol. 8, 1990, pp. 336–342.

[15]McGuinness, M. D., "Flow With a Separation Bubble: Steady and Unsteady Aspects," Ph.D. Dissertation, Cambridge Univ., Cambridge, England, UK, 1978.

[16]Devenport, W. J., "Separation Bubbles at High Reynolds Number: Measurement and Computation," Ph.D. Dissertation, Cambridge Univ., Cambridge, England, UK, 1985.

[17]Bradbury, L. J. S., and Castro, I. P., "A Pulsed-Wire Technique for Velocity Measurements in Highly Turbulent Flows," *Journal of Fluid Mechanics,* Vol. 49, 1971, pp. 657–691.

[18]Castro, I. P., and Dianat, M., "The Pulsed Wire Skin-Friction Measurement Technique," *5th Symposium on Turbulent Shear Flows,* 1985, Paper 11.19.

[19]Bradbury, L. J. S., "Measurements with a Pulsed-Wire and Hot-Wire Anemometer in the Highly Turbulent Wake of a Normal Flat Plate," *Journal of Fluid Mechanics,* Vol. 77, 1976, pp. 473–497.

[20]Kline, S. J., and McClintock, F. A., "Describing Uncertainties in Single-Sample Experiments," *Mechanical Engineering,* Vol. 75, No. 1, 1953, pp. 3–8.

[21]Driver, D. M., and Seegmiller, H. L., "Features of a Reattaching Turbulent Shear Layer in Divergent Channel Flow," *AIAA Journal,* Vol. 23, No. 2, 1985, pp. 163–171.

[22]Simpson, R. L., "A Model for the Backflow Mean Velocity Profile," *AIAA Journal,* Vol. 21, No. 1, 1983, pp. 142–143.

[23]Simpson, R. L., "Two-Dimensional Turbulent Separated Flow," AGARD AG 287, Vol. 1, 1985.

[24]Lin, C. C., "Motion in the Boundary Layer with a Rapidly Oscillating External Flow," *Proceedings of the 9th International Congress on Applied Mechanics,* Vol. 4, 1957, pp. 155–167.

[25]Schlichting, H., *Boundary-Layer Theory,* McGraw-Hill, New York, 1960.

[26]Cherry, N. J., "The Effects of Stream Turbulence on a Separated Flow with Reattachment," Ph.D. Dissertation, Imperial College, Univ. of London, England, UK, 1982.